

Linear correlations between ^4He trimer and tetramer energies calculated with various realistic ^4He potentials

E. Hiyama*

RIKEN Nishina Center, RIKEN, Wako 351-0198, Japan

M. Kamimura†

Department of Physics, Kyushu University, Fukuoka 812-8581, Japan,
and RIKEN Nishina Center, RIKEN, Wako 351-0198, Japan

(Dated: November 2, 2018)

In a previous work [Phys. Rev. A **85**, 022502 (2012)] we calculated, with the use of the Gaussian expansion method for few-body systems, the energy levels and spatial structures of the ^4He trimer and tetramer ground and excited states using the LM2M2 potential, which has a very strong short-range repulsion. In this work, we calculate the same quantities using the current most accurate ^4He - ^4He potential [M. Przybytek *et al.*, Phys. Rev. Lett. **104**, 183003 (2010)] that includes the adiabatic, relativistic, QED and residual retardation corrections. Contributions of the corrections to the tetramer ground-(excited-)state energy -573.90 (-132.70) mK are respectively -4.13 (-1.52) mK, $+9.37$ ($+3.48$) mK, -1.20 (-0.46) mK and $+0.16$ ($+0.07$) mK. Further including other realistic ^4He potentials, we calculated the binding energies of the trimer and tetramer ground and excited states, $B_3^{(0)}$, $B_3^{(1)}$, $B_4^{(0)}$ and $B_4^{(1)}$, respectively. We found that the four kinds of the binding energies for the different potentials exhibit perfect linear correlations between any two of them over the range of binding energies relevant for ^4He atoms (namely, six types of the generalized Tjon lines are observed). The dimerlike-pair model for ^4He clusters, proposed in the previous work, predicts a simple interaction-independent relation $\frac{B_4^{(1)}}{B_2} = \frac{B_3^{(0)}}{B_2} + \frac{2}{3}$, which precisely explains the correlation between the tetramer excited-state energy and the trimer ground-state energy, with B_2 being the dimer binding energy.

I. INTRODUCTION

The bosonic $J = 0^+$ three and four ^4He atom systems, which are very weakly bound under the ^4He - ^4He potential with an extremely strong repulsive core followed by the van der Waals attraction, are known to be suitable for studying the Efimov effect and the universality in the systems interacting with large scattering length [1–5].

In a previous paper [6], referred to as paper I in the following, we presented state-of-the-art four-body calculations for the ^4He tetramer ground- and excited-state binding energies and structural properties using a realistic ^4He potential called LM2M2 [7], which has a very strong short-range repulsion. At the same time, our three-body calculation reproduced all the well known results for the ^4He trimer. We took the Gaussian expansion method (GEM) for *ab initio* variational calculations of few-body systems [8–10]. The total wave function is expanded in terms of totally symmetrized few-body Gaussian basis functions, ranging from very compact to very diffuse with the Gaussian ranges in geometric sequences.

The method is suitable for describing the short-range correlations (without *a priori* assumption of any two-body correlation function) and the long-range asymptotic behavior (see the review papers [10–13] for many applications of the GEM). As a result, we found in paper I that precisely the same shapes of the short-range correlation ($r_{ij} \lesssim 4\text{Å}$) in the dimer appear in the ground and excited states of the trimer and tetramer

and that the wave functions of the very weakly-bound excited states of the trimer and the tetramer reproduce the correct asymptotic behavior up to up to $\sim 1000\text{Å}$.

Recently, Przybytek *et al.* [14] proposed a ^4He pair potential that is currently most accurate. Such an accurate ^4He potential is of importance, according to Ref. [14], in several branches of science, for example, in metrology (thermodynamics standards) [15–17], helium-nanodroplet spectroscopy [18, 19], and low-temperature condensed matter physics [20] as well as in the study of the unusually large and very weakly bound states of the ^4He clusters. The potential of Ref. [14] includes, in addition to the standard Born-Oppenheimer (BO) potential, various post-BO contributions. The main contributions are (i) the adiabatic corrections resulting from the leading-order coupling of the electronic and nuclear motions, (ii) the relativistic corrections to the Schrödinger equation, (iii) the quantum electrodynamics (QED) corrections, and (iv) the residual retardation correction. The largest contribution to the dimer energy (-1.615 mK) is $+0.226$ mK repulsively from the correction (ii), and the total contribution is $+0.103$ mK with a mutual cancellation among (i)–(iv) [14]. The potential is referred to as “PCKLJS” (an acronym for Przybytek-Cencek-Komasa-Lach-Jeziorski-Szalewicz, the authors of Ref. [14]) in a subsequent paper [21]; hereafter we use this acronym.

The first purpose of the present work is to calculate, using the potential PCKLJS, the binding energies of the trimer and tetramer ground and excited states, $B_3^{(0)}$, $B_3^{(1)}$, $B_4^{(0)}$ and $B_4^{(1)}$, respectively, together with the estimation of the individual contributions of the corrections (i)–(iv).

The large scattering length of ^4He - ^4He potential leads to universal properties in the four-body problem. An exam-

*Electronic address: hiyama@riken.jp

†Electronic address: mkamimura@riken.jp

ple is existence of the correlations between the different observables. Thus, the second purpose of this work is to calculate the binding energies $B_3^{(0)}, B_3^{(1)}, B_4^{(0)}$ and $B_4^{(1)}$ using various realistic ${}^4\text{He}$ potentials and investigate six types of the correlations between any two of the four energies. The potentials employed are PCKLJS and six other potentials: LM2M2 [7], TTY [22], HFD-B [23], HFD-B3-FCI1 [24–26], SAPT96 [26–28] and CCSAPT07 [29] (see Ref. [30] for a review of the recent study of the ${}^4\text{He}$ potential); in the last three, we choose the cases of the retardation corrections included.

Recently, universal correlations between observables have been studied extensively in four-boson systems interacting with large scattering length [5, 31–36]. As for the specific ${}^4\text{He}$ tetramers, the universal scaling functions for the correlations between the trimer and tetramer binding energies were obtained by the leading-order effective theory [4, 5] and compared with the energies calculated using realistic ${}^4\text{He}$ potentials. However, due to the scarce calculation of the ${}^4\text{He}$ tetramer excited-state binding energy $B_4^{(1)}$ using the realistic pair potential at that time, the correlations associated with $B_4^{(1)}$ remained unexplored (see Fig. 4 of Ref. [5]). In the present work, we provide precise systematic results on the six types of correlations and demonstrate that the correlations are all linear over the range of binding energies relevant to ${}^4\text{He}$ atoms. We compare the result with that given by the leading-order effective theory [4, 5] for ${}^4\text{He}$ atoms.

This paper is organized as follows: In Sec. II, we briefly present our calculational method GEM [8–10]. Calculated results using the PCKLJS potential are presented in Sec. III together with those for the post-BO corrections (i)–(iv). In Sec. IV, using various ${}^4\text{He}$ potentials, we calculate the trimer and tetramer ground- and excited-state binding energies and discuss the correlations between them in comparison with the universal scaling functions obtained by the leading-order effective theory for the ${}^4\text{He}$ atom. A summary is given in Sec. V.

II. METHOD

We employ the same *ab initio* variational method GEM as in the previous work [6] to solve the ground and excited states of the ${}^4\text{He}$ trimer and tetramer. Here, we review the method for the case of the tetramer.

We take two types of Jacobi coordinate sets, K -type and H -type (Fig. 1). For the K -type, $\mathbf{x}_1 = \mathbf{r}_2 - \mathbf{r}_1$, $\mathbf{y}_1 = \mathbf{r}_3 - \frac{1}{2}(\mathbf{r}_1 + \mathbf{r}_2)$ and $\mathbf{z}_1 = \mathbf{r}_4 - \frac{1}{3}(\mathbf{r}_1 + \mathbf{r}_2 + \mathbf{r}_3)$ and cyclically for $\{\mathbf{x}_i, \mathbf{y}_i, \mathbf{z}_i; i = 2, \dots, 12\}$ by the symmetrization between the four particles. For the H -type, $\mathbf{x}_{13} = \mathbf{r}_2 - \mathbf{r}_1$, $\mathbf{y}_{13} = \mathbf{r}_4 - \mathbf{r}_3$, and $\mathbf{z}_{13} = \frac{1}{2}(\mathbf{r}_3 + \mathbf{r}_4) - \frac{1}{2}(\mathbf{r}_1 + \mathbf{r}_2)$ and cyclically for $\{\mathbf{x}_i, \mathbf{y}_i, \mathbf{z}_i; i = 14, \dots, 18\}$.

The total four-body wave function Ψ_4 is to be obtained by solving the Schrödinger equation

$$(H - E)\Psi_4 = 0 \quad (2.1)$$

with the Hamiltonian

$$H = -\frac{\hbar^2}{2\mu_x}\nabla_x^2 - \frac{\hbar^2}{2\mu_y}\nabla_y^2 - \frac{\hbar^2}{2\mu_z}\nabla_z^2 + \sum_{1=i<j}^4 V(r_{ij}), \quad (2.2)$$

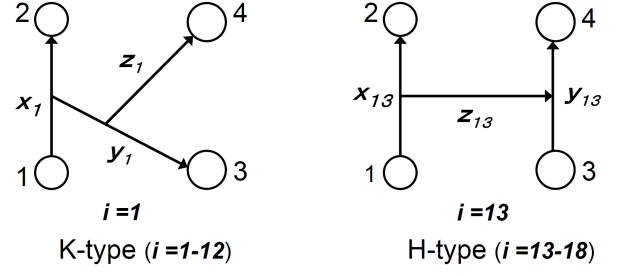


FIG. 1: K -type and H -type Jacobi coordinates for the ${}^4\text{He}$ tetramer. Symmetrization of the four particles generates the sets $i = 1, \dots, 12$ (K -type) and $i = 13, \dots, 18$ (H -type).

where $\mu_x = \frac{1}{2}m$, $\mu_y = \frac{2}{3}m$ and $\mu_z = \frac{3}{4}m$ on the K -type coordinates, and $\mu_x = \mu_y = \frac{1}{2}m$ and $\mu_z = m$ on the H -type ones, m being the mass of the ${}^4\text{He}$ atom. We take $\frac{\hbar^2}{m} = 12.11928 \text{ K}\text{\AA}^2$ [37]. $V(r_{ij})$ is the two-body ${}^4\text{He}$ - ${}^4\text{He}$ potential as a function of the pair separation $\mathbf{r}_{ij} = \mathbf{r}_j - \mathbf{r}_i$.

The wave function Ψ_4 is expanded in terms of the symmetrized L^2 -integrable K -type and H -type four-body basis functions:

$$\Psi_4 = \sum_{\alpha_K=1}^{\alpha_K^{\max}} A_{\alpha_K}^{(K)} \Phi_{\alpha_K}^{(\text{sym};K)} + \sum_{\alpha_H=1}^{\alpha_H^{\max}} A_{\alpha_H}^{(H)} \Phi_{\alpha_H}^{(\text{sym};H)}, \quad (2.3)$$

$$\Phi_{\alpha_K}^{(\text{sym};K)} = \sum_{i=1}^{12} \Phi_{\alpha_K}^{(K)}(\mathbf{x}_i, \mathbf{y}_i, \mathbf{z}_i), \quad (2.4)$$

$$\Phi_{\alpha_H}^{(\text{sym};H)} = \sum_{i=13}^{18} \Phi_{\alpha_H}^{(H)}(\mathbf{x}_i, \mathbf{y}_i, \mathbf{z}_i), \quad (2.5)$$

in which $(\mathbf{x}_i, \mathbf{y}_i, \mathbf{z}_i)$ is the i -th set of Jacobi coordinates. It is of importance that $\Phi_{\alpha_K}^{(\text{sym};K)}$ and $\Phi_{\alpha_H}^{(\text{sym};H)}$ are constructed on the full 18 sets of Jacobi coordinates; this makes the function space of the basis quite wide.

The eigenenergies E and amplitudes $A_{\alpha_K}^{(K)}$ ($A_{\alpha_H}^{(H)}$) are determined by the Rayleigh-Ritz variational principle:

$$\langle \Phi_{\alpha_K}^{(\text{sym};K)} | H - E | \Psi_4 \rangle = 0, \quad (2.6)$$

$$\langle \Phi_{\alpha_H}^{(\text{sym};H)} | H - E | \Psi_4 \rangle = 0, \quad (2.7)$$

where $\alpha_K = 1, \dots, \alpha_K^{\max}$ and $\alpha_H = 1, \dots, \alpha_H^{\max}$. These equations result in the generalized matrix eigenvalue problem [Eqs.(3.8)–(3.10) of paper I].

We describe the basis function $\Phi_{\alpha_K}^{(K)}$ ($\Phi_{\alpha_H}^{(H)}$) in the form

$$\begin{aligned} \Phi_{\alpha_K}^{(K)}(\mathbf{x}_i, \mathbf{y}_i, \mathbf{z}_i) &= \phi_{n_x l_x}^{(\cos)}(x_i) \phi_{n_y l_y}(y_i) \varphi_{n_z l_z}(z_i) \\ &\quad \times \left[[Y_{l_x}(\hat{\mathbf{x}}_i) Y_{l_y}(\hat{\mathbf{y}}_i)]_{\Lambda} Y_{l_z}(\hat{\mathbf{z}}_i) \right]_{JM}, \\ &\quad (i = 1, \dots, 12) \end{aligned} \quad (2.8)$$

$$\begin{aligned} \Phi_{\alpha_H}^{(H)}(\mathbf{x}_i, \mathbf{y}_i, \mathbf{z}_i) &= \phi_{n_x l_x}^{(\cos)}(x_i) \psi_{n_y l_y}(y_i) \varphi_{n_z l_z}(z_i) \\ &\quad \times \left[[Y_{l_x}(\hat{\mathbf{x}}_i) Y_{l_y}(\hat{\mathbf{y}}_i)]_{\Lambda} Y_{l_z}(\hat{\mathbf{z}}_i) \right]_{JM}, \\ &\quad (i = 13, \dots, 18) \end{aligned} \quad (2.9)$$

where α_K specifies the set

$$\alpha_K \equiv \{\cos \text{ or } \sin, \omega, n_x l_x, n_y l_y, n_z l_z, \Lambda, JM\}, \quad (2.10)$$

which is the same for the components $i = 1, \dots, 12$; and similarly for α_H , for all $i = 13, \dots, 18$. J is the total angular momentum and M is its z component. In this paper, we consider the tetramer bound states with $J = 0$. Therefore, the totally symmetric four-body wave function requires (i) $l_x = \text{even}$, $l_y + l_z = \text{even}$ and $\Lambda = l_z$ for the K -type basis and (ii) $l_x = \text{even}$, $l_y = \text{even}$ and $\Lambda = l_z = \text{even}$ for the H -type basis.

In Eqs. (2.8) and (2.9), the radial functions are assumed as

$$\phi_{n_x l_x}^{(\cos)}(x) = x^{l_x} e^{-(x/x_{n_x})^2} \times \begin{cases} \cos \omega(x/x_{n_x})^2 \\ \sin \omega(x/x_{n_x})^2 \end{cases}, \quad (2.11)$$

$$\psi_{n_y l_y}(y) = y^{l_y} e^{-(y/y_{n_y})^2}, \quad (2.12)$$

$$\varphi_{n_z l_z}(z) = z^{l_z} e^{-(z/z_{n_z})^2} \quad (2.13)$$

with geometric sequences of the Gaussian ranges:

$$x_{n_x} = x_1 a_x^{n_x - 1} \quad (n_x = 1, \dots, n_x^{\max}), \quad (2.14)$$

$$y_{n_y} = y_1 a_y^{n_y - 1} \quad (n_y = 1, \dots, n_y^{\max}), \quad (2.15)$$

$$z_{n_z} = z_1 a_z^{n_z - 1} \quad (n_z = 1, \dots, n_z^{\max}). \quad (2.16)$$

It should be emphasized that the GEM few-body calculations need neither the introduction of any *a priori* pair correlation function (such as the Jastrow function) nor separation of the coordinate space into $x < r_c$ and $x > r_c$, with r_c being the radius of a strongly repulsive core potential. Proper short-range correlation and asymptotic behavior of the total wave function are *automatically* obtained by solving the Schrödinger equation (2.1) using the above basis functions for *ab initio* calculations.

We take the same three- and four-body Gaussian basis functions as those employed in paper I. The numbers of the total bases are 4400 for the trimer and 29056 for the tetramer; the bases range from very compact to very diffuse with the Gaussian ranges in geometric sequences.

III. THE PCKLJS POTENTIAL AND ^4He TRIMER AND TETRAMER

The currently most accurate *ab initio* potential, the PCKLJS [14] potential, is given as a function of the ^4He pair separation distance r by

$$V(r) = V_{\text{BO}}(r) + V_{\text{ad}}(r) + V_{\text{rel}}(r) + V_{\text{QED}}(r), \quad (3.1)$$

which are composed of the nonrelativistic BO potential (V_{BO}) and the leading order coupling of the electronic and nuclear motions, that is, the adiabatic correction (V_{ad}), relativistic corrections (V_{rel}), and quantum electrodynamics corrections (V_{QED}). Besides them the Casimir-Polder retardation effect [38], denoted as $V_{\text{ret}}(r)$, can be optionally added to $V(r)$. By the PCKLJS potential we mean the full $V(r)$ plus the

residual retardation correction $V_{\text{ret}}(r)$. Contributions of the individual corrections are discussed in Sec.IIIA.

Use of PCKLJS for the dimer [14] gives the binding energy $B_2 = 1.62 \pm 0.03$ mK, the average separation $\langle r \rangle = 47.1 \pm 0.5$ Å and the s -wave scattering length $a = 90.42 \pm 0.92$ Å. Experimental values of the quantities were reported [39] as $B_2 = 1.1_{-0.2}^{+0.3}$ mK, $\langle r \rangle = 52 \pm 4$ Å and $a = 104_{-18}^{+8}$ Å, but the B_2 and a were calculated [39] from the observed value of $\langle r \rangle$ using rather crude models: $B_2 = \hbar^2/(4m\langle r \rangle^2)$ and $a = 2\langle r \rangle$, where m is mass of ^4He atom. Much better estimates of what should be the values of B_2 and a corresponding to the experimental $\langle r \rangle$ were recently obtained in Ref. [40], a follow-up paper to Ref. [14], to be $B_2 = 1.3_{-0.19}^{+0.25}$ mK and $a = 100.2_{-7.9}^{+8.0}$ Å, which are substantially close to and nearly consistent with the *ab initio* results [14] mentioned above.

Calculated binding energies of the trimer and tetramer for the PCKLJS potential are $B_3^{(0)} = 131.84$ mK, $B_3^{(1)} = 2.6502$ mK (1.03 mK below the dimer), and $B_4^{(0)} = 573.90$ mK, $B_4^{(1)} = 132.70$ mK (0.86 mK below the trimer ground state). Some of the mean values of the trimer (tetramer) ground and excited states, as well as the binding energies mentioned above are summarized in Table I (Table II). The PCKLJS potential gives slightly deeper binding of the trimer and tetramer than the LM2M2 potential does [6].

A. Spatial structure of the tetramer

We discuss the spatial structure of the tetramer excited state. In the study of four-boson states and their connection to the Efimov physics, the authors of Refs. [31, 32] predicted that below each Efimov trimer a pair of tetramer states ($J^\pi = 0^+$) should exist and that the shallower member of the lowest-lying pair is dominantly composed of the ground-state trimer and a distant atom. It is shown, in the calculations by Lazauskas and Carbonell [42] and by the present authors [6] using the realistic LM2M2 potential, that the above prediction is realized in the two bound states of the ^4He tetramer below the trimer ground state.

The structure of the ^4He tetramer excited state is seen essentially in Fig. 2 for the overlap function $\mathcal{O}_4^{(v)}(z)$ between a tetramer state $\Psi_4^{(v)}(v = 0, 1)$ and the trimer ground state $\Psi_3^{(0)}$ which is defined as a function of the distance z between the trimer and the fourth atom:

$$\mathcal{O}_4^{(v)}(z_1) Y_{00}(\hat{\mathbf{z}}_1) = \langle \Psi_3^{(0)} | \Psi_4^{(v)} \rangle_{\mathbf{x}_1, \mathbf{y}_1}. \quad (3.2)$$

Figure 2 indicates that the fourth atom is located in the trimer core region in the tetramer ground state but is far from the trimer in the excited state. This is also understood from the fact that, in Tables I and II, the binding energy and the quantities $\langle T \rangle$ and $\langle V \rangle$ for the tetramer excited state are very close to those for the trimer ground state.

TABLE I: The binding energies $B_3^{(v)}$ ($v = 0, 1$) and mean values of the ^4He trimer ground and excited states using the PCKLJS potential [14] including all the corrections. r_{ij} stands for interparticle distance and r_{iG} is the distance of a particle from the center of mass of the trimer. $C_3^{(v)}$ is the asymptotic normalization coefficient defined by Eq.(2.25) in paper I. The conversion constant $\frac{\hbar^2}{m} = 12.11928 \text{ K}\text{\AA}^2$ is taken.

Trimer (PCKLJS)	Ground state ($v = 0$)	Excited state ($v = 1$)
$B_3^{(v)}$ (mK)	131.84	2.6502
$\langle T \rangle$ (mK)	1694.0	132.0
$\langle V \rangle$ (mK)	-1825.8	-134.7
$\sqrt{\langle r_{ij}^2 \rangle}$ (Å)	10.83	100.4
$\langle r_{ij} \rangle$ (Å)	9.53	81.15
$\langle r_{ij}^{-1} \rangle$ (Å $^{-1}$)	0.136	0.0276
$\langle r_{ij}^{-2} \rangle$ (Å $^{-2}$)	0.0231	0.00231
$\sqrt{\langle r_{iG}^2 \rangle}$ (Å)	6.254	57.95
$C_3^{(v)}$ (Å $^{-1/2}$)	0.592	0.178

TABLE II: The binding energies $B_4^{(v)}$ ($v = 0, 1$) and mean values of the ^4He tetramer ground and excited states using the PCKLJS potential [14] including all the corrections. r_{ij} stands for interparticle distance and r_{iG} is the distance of a particle from the center-of-mass of the tetramer. $C_4^{(v)}$ is the asymptotic normalization coefficient defined by Eq.(3.22) in paper I. The conversion constant $\frac{\hbar^2}{m} = 12.11928 \text{ K}\text{\AA}^2$ is taken.

Tetramer (PCKLJS)	Ground state ($v = 0$)	Excited state ($v = 1$)
$B_4^{(v)}$ (mK)	573.90	132.70
$\langle T \rangle$ (mK)	4340.4	1673.4
$\langle V \rangle$ (mK)	-4914.3	-1806.1
$\sqrt{\langle r_{ij}^2 \rangle}$ (Å)	8.35	54.5
$\langle r_{ij} \rangle$ (Å)	7.65	35.8
$\langle r_{ij}^{-1} \rangle$ (Å $^{-1}$)	0.156	0.0797
$\langle r_{ij}^{-2} \rangle$ (Å $^{-2}$)	0.0288	0.0119
$\sqrt{\langle r_{iG}^2 \rangle}$ (Å)	5.12	33.0
$C_4^{(v)}$ (Å $^{-1/2}$)	2.1	0.10

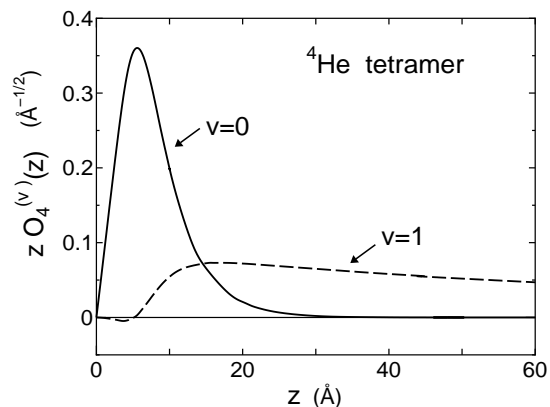


FIG. 2: Overlap function $O_4^{(v)}(z)$ in Eq. (3.2) between the tetramer state ($v = 0, 1$) and the trimer ground state as a function of the atom-trimer distance z .

B. Relativistic and QED corrections

The first four columns of Table III list the calculated dimer binding energy and the average interparticle distance at each level of theory [PCKLJS (a) to (h)], showing the contributions of V_{BO} , V_{ad} , V_{rel} , V_{QED} and the retardation corrections (denoted as “r.c.”), which are different at different levels of theory [48]. The numbers in the first and second columns, given by Ref. [14], are precisely reproduced by our calculation.

Using the potentials PCKLJS (a) to (h), we calculated the binding energies of the ground and excited states of the ^4He trimer and tetramer, $B_3^{(0)}$, $B_3^{(1)}$, $B_4^{(0)}$ and $B_4^{(1)}$, which are listed in Table III. In the tetramer ground-(excited)-state en-

ergy, $-B_4^{(0)}$ ($-B_4^{(1)}$), the contribution from each correction is as follows: The retardation correction is $+6.87$ ($+2.55$) mK repulsively for V_{BO} , but the residual (remaining) correction is only $+0.16$ ($+0.07$) mK for $V_{\text{BO}} + V_{\text{ad}} + V_{\text{rel}} + V_{\text{QED}}$. Comparing (a) and (c), we see that the nonadiabatic correction (V_{ad}) is -4.13 (-1.52) mK attractively. From (c) and (e), the relativistic correction (V_{rel}) is known as $+9.37$ ($+3.48$) mK. The QED correction (V_{QED}) is -1.20 (-0.46) mK from (e) and (g); the entire correction amounts to $+4.20$ ($+1.57$) mK.

We remark that each correction for the tetramer excited-state energy ($-B_4^{(1)}$) is approximately the same as the corresponding correction for the trimer ground-state energy ($-B_3^{(0)}$). For example, the difference between (e) and (g), the QED correction, is -0.46 (-0.46) mK and that between (a) and (h), the full correction, is $+1.57$ ($+1.59$) mK for $-B_4^{(1)}$ ($-B_3^{(0)}$). This is quite reasonable since the same explanation in the paragraph below Eq. (3.2) is applicable. A similar tendency is seen in the comparison between the correction for the trimer excited-state energy ($-B_3^{(1)}$) and that for the dimer ($-B_2$); for example, the QED correction is -0.036 (-0.030) mK and the full correction is $+0.12$ ($+0.10$) mK for $-B_3^{(1)}$ ($-B_2$).

IV. UNIVERSALITY IN ^4He TRIMER AND TETRAMER

Universal correlations between observables have been studied systematically in four-boson systems interacting with large scattering length [5, 31–36]. In this section we investigate the correlations between the ground- and excited-state binding energies of the ^4He trimer and tetramer. We calculate the energies using various realistic ^4He - ^4He interac-

TABLE III: Calculated binding energies of the ^4He dimer, trimer and tetramer using the PCKLJS potential [14] to demonstrate the contributions of V_{BO} , V_{ad} , V_{rel} , V_{QED} and the retardation correction, denoted as "r.c.", appropriate for a given level of theory. PCKLJS-h is the full PCKLJS potential. B_2 and $\langle r \rangle$ are the binding energy and the average separation of the dimer, respectively. Calculated results for the dimer by Ref. [14] are shown in the first and second columns. The conversion constant $\frac{\hbar^2}{m} = 12.11928 \text{ K}\text{\AA}^2$ is taken.

PCKLJS potential [14]	Dimer [14]		Dimer		Trimer		Tetramer	
	B_2 (mK)	$\langle r \rangle$ (\AA)	B_2 (mK)	$\langle r \rangle$ (\AA)	$B_3^{(0)}$ (mK)	$B_3^{(1)}$ (mK)	$B_4^{(0)}$ (mK)	$B_4^{(1)}$ (mK)
(a) V_{BO}	1.718	45.77	1.7181	45.77	133.43	2.7724	578.10	134.27
(b) $V_{\text{BO}} + \text{r.c.}$	1.555	47.92	1.5549	47.92	130.85	2.5776	571.23	131.72
(c) $V_{\text{BO}} + V_{\text{ad}}$	1.816	44.62	1.8160	44.62	134.96	2.8881	582.23	135.79
(d) $V_{\text{BO}} + V_{\text{ad}} + \text{r.c.}$	1.648	46.65	1.6482	46.65	132.37	2.6894	575.33	133.23
(e) $V_{\text{BO}} + V_{\text{ad}} + V_{\text{rel}}$	1.590	47.43	1.5896	47.43	131.44	2.6194	572.86	132.31
(f) $V_{\text{BO}} + V_{\text{ad}} + V_{\text{rel}} + \text{r.c.}$	1.611	47.15	1.6105	47.15	131.76	2.6444	573.69	132.62
(g) $V_{\text{BO}} + V_{\text{ad}} + V_{\text{rel}} + V_{\text{QED}}$	1.620	47.02	1.6200	47.02	131.90	2.6559	574.06	132.77
(h) $V_{\text{BO}} + V_{\text{ad}} + V_{\text{rel}} + V_{\text{QED}} + \text{r.c.}$	1.615	47.09	1.6154	47.09	131.84	2.6502	573.90	132.70

TABLE IV: The binding energy B_2 and the average interparticle distance $\langle r \rangle$ of the dimer calculated using the seven ^4He potentials. The conversion constant $\frac{\hbar^2}{m} = 12.11928 \text{ K}\text{\AA}^2$ is taken. The values reported in the literature are also shown, but the numbers in the parentheses were obtained by using $\frac{\hbar^2}{m} = 12.12 \text{ K}\text{\AA}^2$ and those in the square brackets were given with the use of the ^4He nuclear mass for m . The potential names are arranged in the increasing order of B_2 .

Potential	This work		Other work		Ref.
	B_2 (mK)	$\langle r \rangle$ (\AA)	B_2 (mK)	$\langle r \rangle$ (\AA)	
LM2M2	1.3094	51.87	(1.3035)	(52.00)	[6]
TTY	1.3156	51.76	(1.3096)	(51.89)	[41]
HFD-B3-FCI1	1.4475	49.52	1.448	49.52	[21]
CCSAPT07	1.5643	47.78	1.56	47.8	[29]
PCKLJS	1.6154	47.09	1.615	47.09	[14]
HFD-B	1.6921	46.07	(1.6854)	(46.18)	[41]
SAPT96	1.7443	45.45	[1.713]	[45.8]	[28]

tions which include the PCKLJS potential and six other potentials LM2M2, TTY, HFD-B, HFD-B3-FCI1, SAPT96 and CCSAPT07 mentioned in Sec. I; in the last three, we choose the cases in which the retardation corrections are included.

We first calculated, using the seven potentials, the binding energy B_2 and the average interparticle distance $\langle r \rangle$ of the dimer and listed them in Table IV together with the values reported in the literature. The scattering lengths are not listed, but they range between 87.92 \AA [26] for SAPT96 and 100.23

TABLE V: The binding energies of ^4He trimer and tetramer ground and excited states calculated with the use of the seven ^4He potentials. The conversion constant $\frac{\hbar^2}{m} = 12.11928 \text{ K}\text{\AA}^2$ is taken.

Potential	Trimer		Tetramer	
	$B_3^{(0)}$ (mK)	$B_3^{(1)}$ (mK)	$B_4^{(0)}$ (mK)	$B_4^{(1)}$ (mK)
LM2M2	126.50	2.2779	559.22	127.42
TTY	126.45	2.2844	558.70	127.37
HFD-B3-FCI1	129.00	2.4475	566.12	129.89
CCSAPT07	131.01	2.5890	571.67	131.88
PCKLJS	131.84	2.6502	573.90	132.70
HFD-B	133.08	2.7420	577.34	133.94
SAPT96	134.02	2.8045	580.01	134.86

\AA [41] for LM2M2 (90.42 \AA [14] for PCKLJS). Here, the names of the seven potentials are arranged from the top to the bottom in the increasing order of B_2 .

The ^4He trimer and tetramer ground- and excited-state binding energies, $B_3^{(0)}$, $B_3^{(1)}$, $B_4^{(0)}$ and $B_4^{(1)}$, are calculated with those potentials and are listed in Table V. The values of each binding energy appear in the increasing order as B_2 does in Table IV except for $B_3^{(0)}$, $B_4^{(0)}$ and $B_4^{(1)}$ for LM2M2 and TTY. This exception is reasonable because TTY is slightly more attractive for $r > 2.65 \text{ \AA}$ than LM2M2, but slightly more repulsive for $r < 2.65 \text{ \AA}$; namely, it is possible that TTY generates larger binding energies than LM2M2 in loosely bound systems (the dimer and the trimer excited

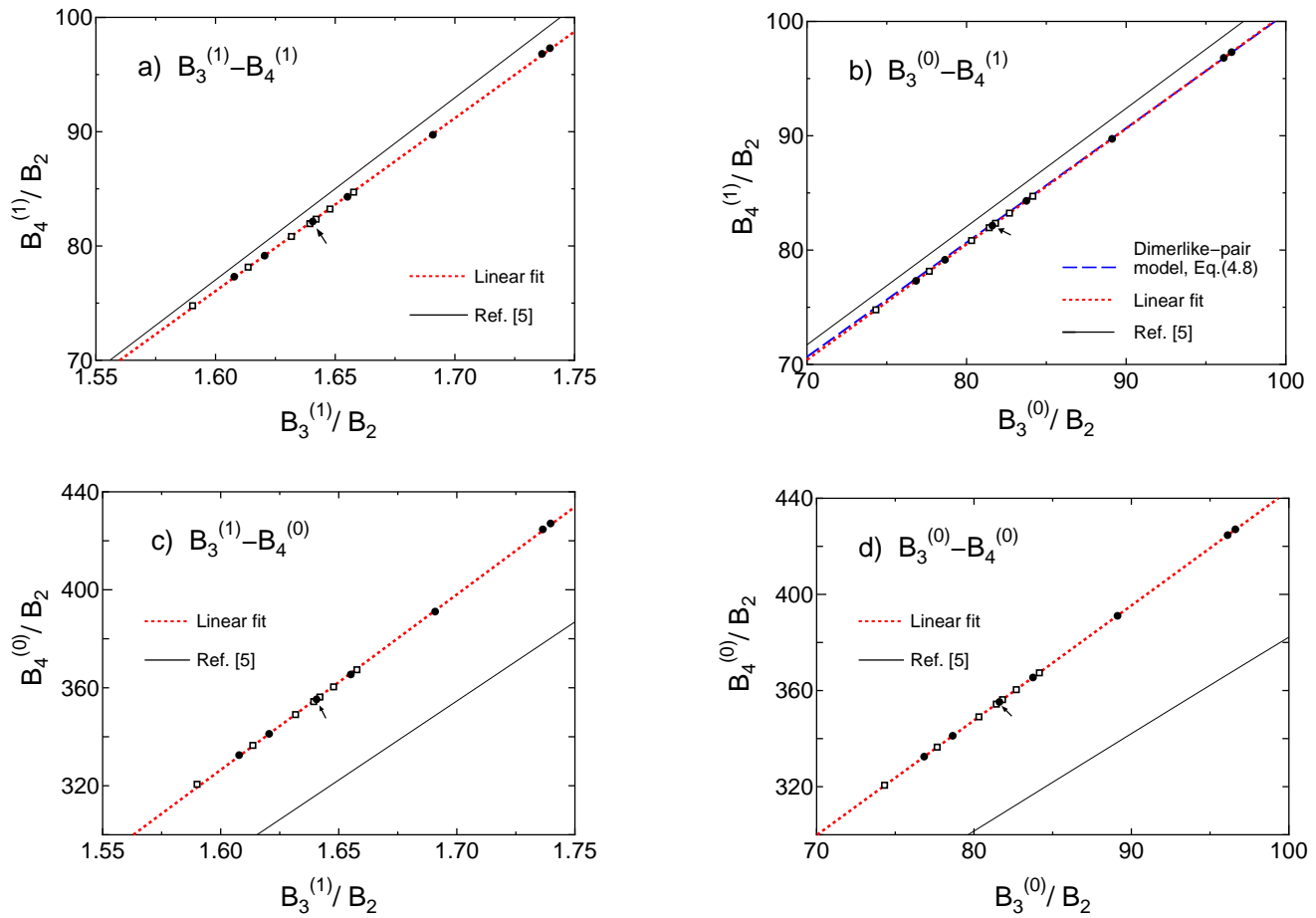


FIG. 3: (Color online). The correlations between the ground- and excited-state binding energies of the ${}^4\text{He}$ trimer and tetramer. (a) $B_3^{(1)} - B_4^{(1)}$, (b) $B_3^{(0)} - B_4^{(1)}$, (c) $B_3^{(1)} - B_4^{(0)}$ and (d) $B_3^{(0)} - B_4^{(0)}$ correlations. The energies are normalized by the dimer energy B_2 . All the 14 data points are obtained by the present calculation for various ${}^4\text{He}$ potentials. The seven closed circles, from the right to the left, denote the results for the seven potentials in Table V from LM2M2 down to SAPT96, respectively; the one designated by an arrow is for PCKLJS. The seven open squares, from the left to the right, show the calculation for each level of the PCKLJS potential in Table I in the order of PCKLJS (c), (a), (d), (g), (f), (e), and (b), respectively. The dotted (red) linear line is the linear least squares fit to the 14 data points; see Eqs. (4.1)–(4.4). The dashed (blue) line in panel (b) is the prediction by the dimerlike-pair model, Eq. (4.8). The solid line, taken from Fig. 4 and Eqs. (39)–(42) in Ref. [5], shows the universal scaling curve obtained by the leading-order effective theory for the ${}^4\text{He}$ trimer and tetramer.

states) but brings about smaller binding energies in compactly bound systems (the trimer and tetramer ground states and the tetramer excited state that is dominantly composed of the compact trimer ground state and a distant ${}^4\text{He}$ atom). We note that if all the binding energies are normalized by B_2 , they appear in the increasing order in Table V.

A. Linear correlations

Correlations between the binding energies in three- and four-body systems were first observed in nuclear physics and are known as the Tjon line [43], which refers to the approximately linear correlation between the binding energies of the triton and the α particle for various nucleon-nucleon potentials. Recently, the nuclear Tjon line was discussed in the context of the effective field theory of short-range interactions

and low-momentum nucleon-nucleon potentials [44, 45]. The Tjon lines for the ${}^4\text{He}$ trimer and tetramers were investigated in Refs. [4, 5] over the range of binding energies relevant to ${}^4\text{He}$ atoms on the basis of the leading-order effective theory. However, due to the scarce calculation of the ${}^4\text{He}$ tetramer excited-state binding energy $B_4^{(1)}$ with the realistic ${}^4\text{He}$ potential at that time, the correlations associated with $B_4^{(1)}$ remained unexplored.

We consider all six kinds of the correlations between two of the four binding energies, $B_3^{(0)}$, $B_3^{(1)}$, $B_4^{(0)}$ and $B_4^{(1)}$, that are calculated using the seven ${}^4\text{He}$ potentials in Table V and the seven potentials of PCKLJS (a) to (g) in Table I. The binding energies are normalized by B_2 , which is different for different ${}^4\text{He}$ potentials; this is due to the fact that the experimental value of the dimer binding energy has not been precisely obtained as mentioned at the beginning of Sec. III.

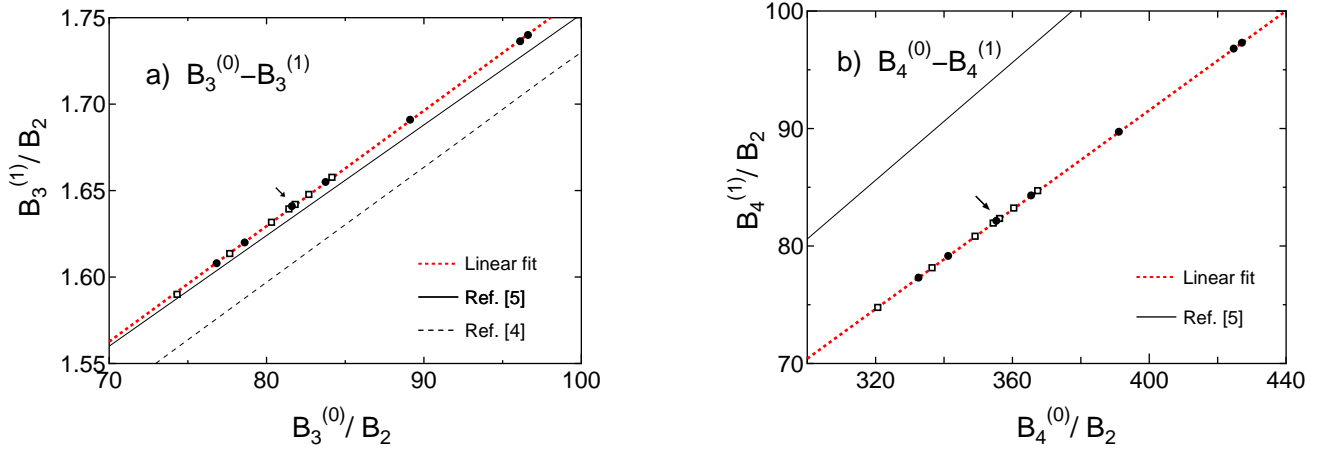


FIG. 4: (Color online). (a) $B_3^{(0)}-B_3^{(1)}$ and (b) $B_4^{(0)}-B_4^{(1)}$ correlations. Meanings of the data points (the present calculation) are the same as in Fig. 3. The dotted (red) linear line is the linear least squares fit to the 14 data points; see Eqs. (4.5) and (4.6). The solid line shows the universal scaling curve obtained by the leading-order effective theory for the ${}^4\text{He}$ atoms; we derived the line from Eqs. (39)–(42) of Ref. [5] (see footnote [49]). The dashed line in (a) is another universal scaling curve obtained in Ref. [4].

Figures 3(a) to 3(d) illustrate the $B_3^{(1)}-B_4^{(1)}$, $B_3^{(0)}-B_4^{(1)}$, $B_3^{(1)}-B_4^{(0)}$ and $B_3^{(0)}-B_4^{(0)}$ correlations, respectively. The 14 data points are given by the present calculation for various 14 potentials mentioned above. The dotted (red) lines in Figs. 3(a) to 3(d) are obtained by the linear least squares fitting to the data points and are represented by the following equations, respectively:

$$\frac{B_4^{(1)}}{B_2} = 151.4 \frac{B_3^{(1)}}{B_2} - 166.1, \quad 70 \lesssim \frac{B_3^{(1)}}{B_2} \lesssim 100, \quad (4.1)$$

$$\frac{B_4^{(1)}}{B_2} = 1.011 \frac{B_3^{(0)}}{B_2} - 0.3694, \quad 1.5 \lesssim \frac{B_3^{(0)}}{B_2} \lesssim 1.8, \quad (4.2)$$

$$\frac{B_4^{(0)}}{B_2} = 715.9 \frac{B_3^{(1)}}{B_2} - 819.0, \quad 70 \lesssim \frac{B_3^{(1)}}{B_2} \lesssim 100, \quad (4.3)$$

$$\frac{B_4^{(0)}}{B_2} = 4.778 \frac{B_3^{(0)}}{B_2} - 34.64, \quad 1.5 \lesssim \frac{B_3^{(0)}}{B_2} \lesssim 1.8. \quad (4.4)$$

Figures 4(a) and 4(b) plot the $B_3^{(0)}-B_3^{(1)}$ and $B_4^{(0)}-B_4^{(1)}$ correlations. With the least squares method, the data points are fitted by the dotted (red) lines that are represented by

$$\frac{B_3^{(1)}}{B_2} = 0.006679 \frac{B_3^{(0)}}{B_2} + 1.095, \quad 70 \lesssim \frac{B_3^{(0)}}{B_2} \lesssim 100, \quad (4.5)$$

$$\frac{B_4^{(1)}}{B_2} = 0.2116 \frac{B_4^{(0)}}{B_2} + 6.961, \quad 300 \lesssim \frac{B_4^{(0)}}{B_2} \lesssim 440. \quad (4.6)$$

In Figs. 3 and 4, the scattering of the data points about the fitted linear line is very small: Representing the data points by $\{(x_i, y_i), i = 1, \dots, 14\}$ and the fitted linear function by $y = f(x)$, we define relative deviation at each x_i by $|y_i - f(x_i)|/y_i$. The average values of the relative deviation in Figs. 3(a), 3(b), ..., 4(b) are respectively 0.093%, 0.0032%,

0.11%, 0.019%, 0.030% and 0.015%. We remark that, among Eqs. (4.1)–(4.6), any three equations can be reproduced by the other three (linearly dependent) with very small errors. This comes from the fact that the six kinds of correlations are all linear for various potentials.

It is unexpected that all the calculated results (the data points) fall so strictly on a straight line over the range of binding energies relevant for ${}^4\text{He}$ atoms; we emphasize that the results are obtained by using *different* potentials, not by changing parameter(s) in a specific potential.

It is of interest to note that the slope of the dotted (red) line in Fig. 3(d) for the correlation between trimer and tetramer ground-state binding energies is 4.778 [see Eq. (4.4)], which is close to the slope of the nuclear Tjon line (≈ 5.0 [44]) for the correlation between three- and four-nucleon binding energies using various nucleon-nucleon potentials.

Another similarity between the ${}^4\text{He}$ tetramer and the ${}^4\text{He}$ nucleus is seen in the comparison of the overlap function $\mathcal{O}_4^{(v)}(z)$ in Fig. 2 (${}^4\text{He}$ tetramer) with that in Fig. 5 (${}^4\text{He}$ nucleus). The behavior of $\mathcal{O}_4^{(v)}(z)$ is quite resemble each other although the sizes of the systems are very different. The first excited 0^+ state of the ${}^4\text{He}$ nucleus is known to be composed of the three-nucleon core and a loosely coupled nucleon [46]. The observed cross sections of the electron inelastic scattering, which drastically excites the compact ground state to the diffuse excited state, is well explained by the GEM four-body calculation by the present authors [46].

In the study of weakly bound four-boson states (not specifically for ${}^4\text{He}$ atoms) at the unitary limit, von Stecher *et al.* [32] obtained $B_4^{(0)}/B_3^{(0)} \approx 4.58$ and $B_4^{(1)}/B_3^{(0)} \approx 1.01$, while Deltuva [47] gave $B_4^{(0)}/B_3^{(0)} \approx 4.611$ and $B_4^{(1)}/B_3^{(0)} \approx 1.0023$, and Hadizadeh *et al.* [35] reported $B_4^{(0)}/B_3^{(0)} \approx 4.6$. In the ${}^4\text{He}$ atoms, we can estimate the ratio, approximately from Eqs. (4.4) and (4.2),

as $B_4^{(0)}/B_3^{(0)} = 4.778 - 34.64B_2/B_3^{(0)} \approx 4.3\text{--}4.4$ and $B_4^{(1)}/B_3^{(0)} = 1.011 - 0.3694 B_2/B_3^{(0)} \approx 1.006\text{--}1.007$ over the range of binding energies relevant for the ${}^4\text{He}$ atoms.

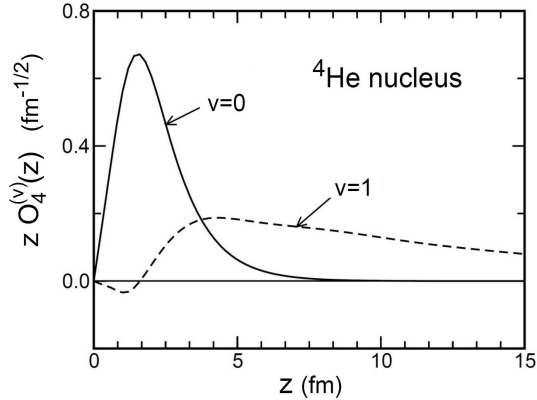


FIG. 5: Overlap function $\mathcal{O}_4^{(v)}(z)$ between the ${}^4\text{He}$ nucleus ($v = 0, 1$) and the three-nucleon ground state as a function of the distance z between the three-nucleon core and the fourth nucleon. Taken from Ref. [46]. Note that this figure is quite similar to Fig. 2 for the ${}^4\text{He}$ tetramer.

B. Universal scaling functions

The solid lines in Fig. 3 illustrate the universal scaling functions relating the tetramer energies to the trimer energies, which were calculated by the leading-order effective theory for the ${}^4\text{He}$ atoms; the lines are taken from Eqs. (39)–(42) and Fig. 4 in Ref. [5]. To obtain the energies, Platter *et al.* [5] constructed an effective ${}^4\text{He}$ - ${}^4\text{He}$ potential including both two- and three-body contact interactions. The two parameters of the effective potential were determined to reproduce the binding energy of the dimer ground state and the trimer excited state. They solved the three- and four-body Faddeev-Yakubovsky equations with the effective potential. Although the $B_3^{(0)}-B_3^{(0)}$ and $B_4^{(0)}-B_4^{(1)}$ correlations are not explicitly given in Ref. [5], we derived the functions for the correlations [49] using Eqs. (39)–(42) in Ref. [5] and plot them in Fig. 4 with the solid lines. The dashed line in Fig. 4(a) is another universal scaling curve for the ${}^4\text{He}$ trimer given in Fig. 2 of Ref. [4].

The solid lines in Figs. 3(a), 3(b) and 4(a), associated with $B_3^{(0)}, B_3^{(1)}$ and $B_4^{(1)}$, are close to the calculated data points. Therefore, origin of the non-negligible deviation of the solid lines in Figs. 3(c) and 3(d) and Fig. 4(b) from the data points is attributed to $B_4^{(0)}$ given by the leading-order effective theory [5]. We estimate that the theory underestimates $B_4^{(0)}$ by some 70–80 mK ($\sim 12\text{--}14\%$ of $B_4^{(0)}$) while it overestimates $B_4^{(1)}$ by about 2–3 mK ($\sim 2\text{--}3\%$ of $B_4^{(1)}$) compared with the calculation using the realistic ${}^4\text{He}$ potentials.

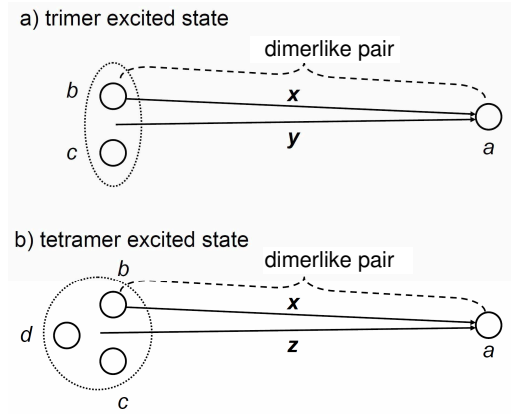


FIG. 6: Schematic picture of the dimerlike-pair model for the trimer and tetramer excited states in the asymptotic region.

C. Dimerlike-pair model

In Fig. 3(b) for the $B_3^{(0)}-B_4^{(1)}$ correlation, the dashed (blue) line, predicted by the dimerlike-pair model [6], is close to the 14 data points with almost the same quality as the dotted (red) line of the least squares fit.

We briefly recapitulate the model. Firstly, for the trimer excited state in Fig. 6(a), the model indicates that (i) particle a , located far from b and c (dimer), which are *loosely* bound, is little affected by the interaction between b and c ; (ii) therefore, the pair a and b at a distance x is asymptotically dimerlike; (iii) since $x \simeq y$ asymptotically, the wave function of particle a along y , $\exp(-k_3^{(1)}y)/y$, is the same as that of the dimer, $\exp(-k_2x)/x$; hence we have a relation $k_3^{(1)} = k_2$. The binding wave numbers are related to the binding energies as

$$k_2 = \sqrt{2\mu_x B_2}/\hbar, \\ k_3^{(1)} = \sqrt{2\mu_y (B_3^{(1)} - B_2)}/\hbar,$$

where $\mu_x = \frac{1}{2}m$ and $\mu_y = \frac{2}{3}m$ are the reduced mass associated with the coordinates \mathbf{x} and \mathbf{y} , respectively. Using the relation $k_3^{(1)} = k_2$, the model predicts

$$\frac{B_3^{(1)}}{B_2} = \frac{B_2}{B_2} + \frac{3}{4} = \frac{7}{4} \quad \left(\frac{\Delta B_3^{(1)}}{B_2} = \frac{3}{4} \right), \quad (4.7)$$

where $\Delta B_3^{(1)} = B_3^{(1)} - B_2$ is the binding energy measured from the dimer.

Similarly, the model predicts the tetramer excited-state energy as follows: Asymptotically, in Fig. 6b, particle a decays from the trimer ($b + c + d$) as $\exp(-k_4^{(1)}z)/z$ with

$$k_4^{(1)} = \sqrt{2\mu_z (B_4^{(1)} - B_3^{(0)})}/\hbar,$$

where $\mu_z = \frac{3}{4}m$ is the reduced atom-trimer mass. Using $k_4^{(1)} = k_2$ by the same reason as above, the model predicts

$$\frac{B_4^{(1)}}{B_2} = \frac{B_3^{(0)}}{B_2} + \frac{2}{3} \quad \left(\frac{\Delta B_4^{(1)}}{B_2} = \frac{2}{3} \right), \quad (4.8)$$

TABLE VI: Comparison of the trimer (tetramer) excited-state binding energy $B_3^{(1)}$ ($B_4^{(1)}$) between the dimerlike-pair-model prediction in the column "model" and the present three-body (four-body) calculation. The model predicts $\frac{\Delta B_3^{(1)}}{B_2} = \frac{3}{4}$ and $\frac{\Delta B_4^{(1)}}{B_2} = \frac{2}{3}$.

Potential	Model		Present calculation			
	$B_3^{(1)}$ (mK)	$B_4^{(1)}$ (mK)	$B_3^{(1)}$ (mK)	$B_4^{(1)}$ (mK)	$\frac{\Delta B_3^{(1)}}{B_2}$	$\frac{\Delta B_4^{(1)}}{B_2}$
LM2M2	2.29	127.37	2.2779	127.42	0.74	0.70
TTY	2.30	127.33	2.2844	127.37	0.74	0.70
HFD-B3-FCI1	2.53	129.96	2.4475	129.89	0.69	0.61
CCSAPT07	2.74	132.05	2.5890	131.88	0.66	0.56
PCKLJS	2.83	132.91	2.6502	132.70	0.64	0.53
HFD-B	2.96	134.21	2.7420	133.94	0.62	0.51
SAPT96	3.05	135.18	2.8045	134.86	0.61	0.48

where $\Delta B_4^{(1)} = B_4^{(1)} - B_3^{(0)}$ is the binding energy measured from the trimer ground state.

We emphasize that the relations (4.7) and (4.8) are interaction independent. Our assumption is only that the interparticle distance in the dimer (trimer) is larger than the interaction range, which is fulfilled in the present case. The relation (4.8) is plotted in Fig. 3(b) by the dashed (blue) line, which almost overlaps with the dotted (red) line for the linear fit to the 14 data points by the present few-body calculation.

The trimer and tetramer excited-state binding energies predicted by the dimerlike-pair model are summarized in Table VI in comparison with the results of the present three- and four-body calculations using various ${}^4\text{He}$ interaction. Error of the model prediction is known to be 0.01–0.25 mK in $B_3^{(1)}$ ($\Delta B_3^{(1)}$) and 0.05–0.32 mK in $B_4^{(1)}$ ($\Delta B_4^{(1)}$) compared with the three-(four-)body calculation. The model works well when we compare, in Fig. 3(b) (the $B_3^{(0)}$ - $B_4^{(1)}$ correlation), the 14 data points with the dashed (blue) line and with the solid line.

However, strictly speaking about the model, it predicts neither $B_3^{(1)}$ ($B_4^{(1)}$) nor the threshold energy B_2 ($B_3^{(0)}$) but does predict their difference $\Delta B_3^{(1)}$ ($\Delta B_4^{(1)}$). Therefore, the error or accuracy of the model prediction might be judged also on the basis of $\Delta B_3^{(1)}$ ($\Delta B_4^{(1)}$). For this purpose, one can compare in Table VI the value of $\frac{\Delta B_3^{(1)}}{B_2}$ ($\frac{\Delta B_4^{(1)}}{B_2}$) by the three-(four-)body calculation with the value, $\frac{3}{4}$ ($\frac{2}{3}$), by the model. The relative error of the model prediction for $\frac{\Delta B_3^{(1)}}{B_2}$ ($\frac{\Delta B_4^{(1)}}{B_2}$) is estimated as 1–19% (5–28%)[50]. This is not very small, but we remark that the simple model provides, without any elaborate calculation, a reason why the quantity $\frac{\Delta B_3^{(1)}}{B_2}$ appears close to $\frac{3}{4}$ (0.61–0.74 in Table VI), and $\frac{\Delta B_4^{(1)}}{B_2}$ is close to $\frac{2}{3}$ (0.48–0.70).

Generally, for the ${}^4\text{He}_N$, the model suggests a relation

$$\frac{B_N^{(1)}}{B_2} = \frac{B_{N-1}^{(0)}}{B_2} + \frac{N}{2(N-1)}, \quad (4.9)$$

where the last term is ratio of the reduced mass of the dimerlike pair ($\frac{1}{2}m$) to that of the ${}^4\text{He}$ - ${}^4\text{He}_{N-1}$ system ($\frac{N-1}{N}m$).

V. SUMMARY

Using the Gaussian expansion method for *ab initio* variational calculations of few-body systems [8–10], we have calculated the binding energies of the ${}^4\text{He}$ trimer and tetramer ground and excited states, $B_3^{(0)}$, $B_3^{(1)}$, $B_4^{(0)}$ and $B_4^{(1)}$, with the use of the currently most accurate ${}^4\text{He}$ potential proposed by Przybytek *et al.* [14], called the PCKLJS potential. This is an extension of our previous work [6] using the LM2M2 potential. Employing the PCKLJS, LM2M2, TTY, HFD-B, HFD-B3-FCI1, SAPT96 and CCSAPT07 potentials, we have calculated the four kinds of the binding energies and investigated the correlations between any two of them.

The main conclusions are summarized as follows:

(i) We obtained, using PCKLJS, $B_3^{(0)} = 131.84$ mK, $B_3^{(1)} = 2.6502$ mK (1.03 mK below the dimer), $B_4^{(0)} = 573.90$ mK and $B_4^{(1)} = 132.70$ mK (0.86 mK below the trimer ground state). This potential includes the adiabatic, relativistic, QED and residual retardation corrections. Contributions of the corrections to the tetramer eigenenergy $-B_4^{(0)}$ ($-B_4^{(1)}$) are, respectively, -4.13 (-1.52) mK, $+9.37$ ($+3.48$) mK, -1.20 (-0.46) mK and $+0.16$ ($+0.07$) mK; the entire correction is $+4.20$ ($+1.57$) mK.

(ii) The six correlations $B_3^{(1)}$ - $B_4^{(1)}$, $B_3^{(0)}$ - $B_4^{(1)}$, $B_3^{(1)}$ - $B_4^{(0)}$, $B_3^{(0)}$ - $B_4^{(0)}$, $B_3^{(0)}$ - $B_3^{(1)}$ and $B_4^{(0)}$ - $B_4^{(1)}$, are observed to be all linear for the various ${}^4\text{He}$ potentials mentioned above over the range of binding energies relevant for the ${}^4\text{He}$ atoms. They may be called the generalized Tjon lines. The universal scaling curves given by the leading-order effective theory for the ${}^4\text{He}$ atoms [5] locate closely to the presently-obtained linear lines in the $B_3^{(0)}$ - $B_4^{(1)}$, $B_3^{(1)}$ - $B_4^{(1)}$ and $B_3^{(0)}$ - $B_3^{(1)}$ correlations, but deviate non-negligibly from the lines in the $B_3^{(0)}$ - $B_4^{(0)}$, $B_3^{(1)}$ - $B_4^{(0)}$ and $B_4^{(0)}$ - $B_4^{(1)}$ correlations. The latter deviations are attributed to the fact that the leading-order effective theory underestimates $B_4^{(0)}$ by some 70–80 mK (~ 12 – 14% of $B_4^{(0)}$) compared with the present calculations using the realistic ${}^4\text{He}$ potentials.

(iii) As long as the binding energies of the excited states of the trimer and tetramer, the interaction-independent prediction, $\frac{B_3^{(1)}}{B_2} = \frac{7}{4}$ and $\frac{B_4^{(1)}}{B_2} = \frac{B_3^{(0)}}{B_2} + \frac{2}{3}$, by the dimerlike-pair model [6] explains the B_2 - $B_3^{(1)}$ and $B_3^{(0)}$ - $B_4^{(1)}$ correlations for the various ${}^4\text{He}$ potentials, with B_2 being the dimer binding energy.

Acknowledgement

We thank Krzysztof Szalewicz for providing us with codes producing the ^4He potential (PCKLJS) used in this

work. The numerical calculations were performed on HITACHI SR16000 at KEK and YIFP.

-
- [1] V. Efimov, *Yad. Fiz.* **12**, 1080 (1970) [*Sov. J. Nucl. Phys.* **12**, 589 (1971)]; *Nucl. Phys. A* **210**, 157 (1973).
- [2] V. Efimov, *Few-Body Syst.* **51**, 79 (2011).
- [3] E. Braaten and H-W. Hammer, *Phys. Reports*, **428**, 259 (2006).
- [4] E. Braaten and H-W. Hammer, *Phys. Rev. A* **67**, 042706 (2003).
- [5] L. Platter, H.-W. Hammer and Ulf-G. Meissner, *Phys. Rev. A* **70**, 052101 (2004).
- [6] E. Hiyama and M. Kamimura, *Phys. Rev. A* **85**, 022502 (2012).
- [7] R.A. Aziz and M.J. Slaman, *J. Chem. Phys.* **94**, 8047 (1991).
- [8] M. Kamimura, *Phys. Rev. A* **38**, 621 (1988).
- [9] H. Kameyama, M. Kamimura and Y. Fukushima, *Phys. Rev. C* **40**, 974 (1989).
- [10] E. Hiyama, Y. Kino and M. Kamimura, *Prog. Part. Nucl. Phys.* **51**, 223 (2003).
- [11] E. Hiyama and T. Yamada, *Prog. Part. Nucl. Phys.* **63**, 339 (2009).
- [12] E. Hiyama *et al.*, *Prog. Theor. Phys. Supplement* **185**, 106 (2010); **185**, 152 (2010).
- [13] E. Hiyama, *Few-Body Systems* **53** (2012), Online First, 14 March, 2012.
- [14] M. Przybytek, W. Cencek, J. Komasa, G. Lach, B. Jeziorski and K. Szalewicz, *Phys. Rev. Lett.* **104**, 183003 (2010); see also the supplementary material at <http://link.aps.org/supplemental/10.1103/PhysRevLett.104.183003> for extended tables and the parameters of the fit.
- [15] J. Fischer and B. Fellmuth, *Rep. Prog. Phys.* **68**, 1043 (2005).
- [16] L. Pitre, M. R. Moldover, and W. L. Tew, *Metrologia* **43**, 142 (2006).
- [17] J. B. Mehl, *Comptes Rendus Physique* **10**, 859 (2009).
- [18] S. Goyal, D. L. Schutt, and G. Scoles, *Phys. Rev. Lett.* **69**, 933 (1992).
- [19] M. Hartmann, R. E. Miller, J. P. Toennies, and A. Vilesov, *Phys. Rev. Lett.* **75**, 1566 (1995).
- [20] S. Y. Chang and M. Boninsegni, *J. Chem. Phys.* **115**, 2629 (2001).
- [21] V. Špirko, S.P.A. Sauer and K. Szalewicz, “On the relation between properties of helium dimer bound state”, preprint (2011).
- [22] K.T. Tang, J.P. Toennies and C.L. Yiu, *Phys. Rev. Lett.* **74**, 1546 (1995).
- [23] R.A. Aziz, F.R.W. McCourt and C.C.K. Wong, *Mol. Chem. Phys.* **61**, 1487 (1987).
- [24] T. van Mourik and J. H. van Lenthe, *J. Chem. Phys.* **102**, 7479 (1995).
- [25] R. A. Aziz, A. R. Janzen, and M. R. Moldover, *Phys. Rev. Lett.* **74**, 1586 (1995).
- [26] A.R. Jansen and R.A. Aziz, *J. Chem. Phys.* **107**, 914 (1997).
- [27] H. L. Williams, T. Korona, R. Bukowski, B. Jeziorski, and K. Szalewicz, *Chem. Phys. Lett.* **262**, 431 (1996).
- [28] T. Korona, H. L. Williams, R. Bukowski, B. Jeziorski, and K. Szalewicz, *J. Chem. Phys.* **106**, 5109 (1997).
- [29] M. Jeziorska, W. Cencek, K. Patkowski, B. Jeziorski, and K. Szalewicz, *J. Chem. Phys.* **127**, 124303 (2007).
- [30] K. Szalewicz, *Int. Rev. Phys. Chem.* **27**, 273 (2008).
- [31] H.-W. Hammer and L. Platter, *Eur. Phys. J. A* **32**, 113 (2007).
- [32] J. von Stecher, J.P. D’Incao and C.H. Greene, *Nature Phys.*, **5**, 417 (2009).
- [33] J.P. D’Incao, J. von Stecher and C.H. Greene, *Phys. Rev. Lett.* **103**, 033004 (2009).
- [34] M.T. Yamashita, L. Tomio, A. Delfino and T. Frederico, *Europhys. Lett.*, **75**, 555 (2006).
- [35] M.R. Hadizadeh, M.T. Yamashita, L. Tomio, A. Delfino and T. Frederico, *Phys. Rev. Lett.*, **107**, 135304 (2011).
- [36] T. Frederico, L. Tomio, A. Delfino, M.R. Hadizadeh and M.T. Yamashita, *Few-Body Syst.*, **51**, 87 (2011).
- [37] V. Roudnev and M. Cavagnero, *J. Phys. B: At. Mol. Opt. Phys.* **45**, 025101 (2012).
- [38] H.B.G. Casimir and D. Polder, *Phys. Rev.* **73**, 360 (1948).
- [39] R. Grisenti *et al.*, *Phys. Rev. Lett.* **85**, 2284 (2000).
- [40] W. Cencek, M. Przybytek, J. Komasa, J.B. Mehl, B. Jeziorski and K. Szalewicz, “Effects of adiabatic, relativistic, and quantum electrodynamics interactions in helium dimer on thermophysical properties of helium”, submitted to *J. Chem. Phys.*(2012) (a follow up paper of Ref. [14]).
- [41] E.A. Kolganova, A.K. Motovilov and W. Sandhas, *Few-Body Syst.* **51**, 249 (2011).
- [42] R. Lazauskas and J. Carbonell, *Phys. Rev. A* **73**, 062717 (2006).
- [43] J.A. Tjon, *Phys. Lett. B* **56**, 217 (1975).
- [44] A. Nogga, S.K. Bogner and A. Schwenk, *Phys. Rev. C* **70**, 061002 (2004).
- [45] L. Platter, H.-W. Hammer and U.-G. Meissner, *Phys. Lett. B* **607**, 254 (2005).
- [46] E. Hiyama, B.F. Gibson and M. Kamimura, *Phys. Rev. C* **70**, 031001(R) (2004).
- [47] A. Deltuva, *Phys. Rev. A* **82**, 040701(R) (2010).
- [48] For example, the retardation correction for V_{BO} is 0.16 mK, but that for $V_{\text{BO}} + V_{\text{ad}} + V_{\text{rel}} + V_{\text{QED}}$ is 0.005 mK in the dimer; namely, the residual contribution becomes much smaller in the latter. See Ref. [14] for the details.
- [49] In Ref. [5], one can obtain an equation to relate $B_3^{(0)}$ and $B_3^{(1)}$ by eliminating $B_4^{(0)}$ from Eqs. (39) and (40) and one more equation from Eqs. (41) and (42) by eliminating $B_4^{(1)}$. Since the resultant two equations are slightly different from each other in the coefficients, we averaged them and obtained $\frac{B_3^{(1)}}{B_2} = 0.006402 \frac{B_3^{(0)}}{B_2} + 1.112$. Similarly, we derived $\frac{B_4^{(1)}}{B_2} = 0.2504 \frac{B_4^{(0)}}{B_2} + 5.480$. They are plotted in Fig. 4 with solid lines
- [50] One sees in Table VI that the error of the model increases with increasing B_2 from the top to the bottom. However, investigation of the reason for this behavior is out of the scope of the present work.